Published in final edited form as:
J Micromech Microeng. 2011 May ; 21(5): 054004–054014. doi:10.1088/0960-1317/21/5/054004.

Capacitive micromachined ultrasonic transducers for medical imaging and therapy

Butrus T. Khuri-Yakub and **Ömer Oralkan**
E. L. Ginzton Laboratory, Center for Nanoscale Science and Engineering, Stanford University, Stanford, CA 94305-4088.

Abstract

Capacitive micromachined ultrasonic transducers (CMUTs) have been subject to extensive research for the last two decades. Although they were initially developed for air-coupled applications, today their main application space is medical imaging and therapy. This paper first presents a brief description of CMUTs, their basic structure, and operating principles. Our progression of developing several generations of fabrication processes is discussed with an emphasis on the advantages and disadvantages of each process. Monolithic and hybrid approaches for integrating CMUTs with supporting integrated circuits are surveyed. Several prototype transducer arrays with integrated frontend electronic circuits we developed and their use for 2-D and 3-D, anatomical and functional imaging, and ablative therapies are described. The presented results prove the CMUT as a MEMS technology for many medical diagnostic and therapeutic applications.

1. Introduction

Microfabricated devices and integrated circuits have great promise for medical applications. Their high level of integration enables complete point-of-care devices at a low cost. These devices also help achieve a compact form factor, higher resolution in imaging and therapy, and higher sensitivity. MEMS technology in general has found commercial success in inertial sensors that are adapted largely by the automotive, the mobile communications, and now by the gaming industries. Display devices, timing references, and microphones are some other product groups MEMS technology has had an impact on. Pressure sensors originally developed for automotive and industrial use represent one of the most widely used MEMS products in the medical field as part of implantable and catheter-based blood pressure monitors. There is also a strong demand for microfluidic devices for medical use. MEMS is increasing its presence in consumer and medical business, adding to its strong base in automotive and industrial applications.

Capacitive micromachined ultrasonic transducers (CMUTs) invented in the mid-1990s [Haller94] have come a long way in the last two decades and recently reached to the market for medical ultrasound imaging [Hitachi09]. Even considering only the production of conventional ultrasonic transducer probes, which amounts to a global market of about $1 billion annually, one can speculate that CMUTs can be the next big MEMS product in the medical field.

In the early years of research in this field the main focus was on basic device fabrication and understanding device operation. Several fabrication processes based on standard surface micromachining techniques have been developed [Jin98, Jin99, Schindel95, Haller96,

khuri-yakub@stanford.edu .

Eccardt96, Eccardt97, Cianci02]. An alternative CMUT fabrication method based on wafer bonding was developed later [Huang03]. Equivalent circuit models for CMUTs have been developed to help with the design of arrays for practical applications [Ladabaum98, Caronti02, Lohfink05]. Finite element analysis (FEA) has been used to understand transducer characteristics (especially crosstalk issues), and to optimize transducer response [Bozkurt99, Wojcik00, Roh02, Yaralioglu05, Bayram07]. 1-D and 2-D array elements have been fully characterized [Oralkan99, Jin01]. Early imaging demonstrations were performed using systems built from discrete electronic components [Oralkan02, Oralkan03]. In this paper, we focus on the more recent developments in CMUT technology including newly introduced fabrication processes, integrated frontend circuits, and their applications in medical imaging and therapy.

The organization of the paper is as follows: the next section briefly describes the basic device structure and the operating principle. In Section 3, the progression of CMUT fabrication processes is summarized. Section 4 details advantages and disadvantages of several approaches to integrate transducer arrays and supporting electronics circuits. Examples of implemented devices for various imaging and therapeutic applications are presented in Section 5 and 6, respectively.

2. CMUT: Basic structure and operating principle

The basic building block of a CMUT is a capacitor cell that consists of a thin movable plate suspended over a vacuum gap. A metal layer on top of the thin plate or the thin plate itself, if conductive, forms the top electrode of the capacitor. The underlying conductive substrate acts as the bottom electrode. When a DC voltage is applied between these two electrodes the top plate is attracted toward the substrate by the electrostatic force. A mechanical restoring force due to the stiffness of the plate resists the attraction. Driving the capacitor with an alternating voltage generates ultrasound. If the movable top plate is subjected to ultrasound pressure, an electrical current is generated due to the capacitance change under constant bias voltage. The amplitude of this current is a function of the frequency of the incident wave, the bias voltage, and the capacitance of the device. The key point to be able to realize a competitive electrostatic transducer is to maintain an electric field in the gap with the strength on the order of 10^8 V/cm or higher. This is also the very reason why MEMS technology was the enabler for this century-old idea of electrostatic transduction for ultrasound generation and detection. As it will be explained in the next section, this high electric field, which makes this device so competitive, also necessitates extreme care in design to avoid any reliability issues related to dielectric charging and breakdown.

The dimensions, the shape, and the mechanical properties of the thin plate mainly determine the operating frequency for the described conventional CMUT structure. Therefore, many capacitor cells are connected in parallel to implement transducers and arrays of transducers in the desired size and shape operating at the desired frequency. For medical use the silicon-based transducer usually is covered by a thin layer of elastic polymer to provide electrical insulation without significantly affecting the performance of the device [Lin10]. One of the major advantages of CMUTs compared to their piezoelectric counterparts is the wide bandwidth. When operated in immersion, the transducer's mechanical plate impedance is much smaller than the loading impedance over a large frequency range, resulting in very broad bandwidth. The lower cutoff frequency is determined by the spring constant. As the spring constant increases, the bandwidth of the transducer decreases. The higher cutoff frequency is determined by the membrane mass and the mass loading of the immersion medium as well as the higher order resonant modes of the plate. Other well-known advantages of MEMS technology such as low cost, amenability to integration with electronic circuits, and miniaturization are all valid for CMUTs as well.

3. CMUT fabrication

Several process flows have been developed by various research groups to implement CMUT arrays by using standard surface and bulk micromachining techniques. This section summarizes some of the CMUT fabrication process flows we developed to progressively address several performance and reliability improvements. The details of these processes are not explained here, but rather the key points are mentioned and the reader is referred to the related literature. Also graphically only the final device structure is depicted for each described process in Fig. 1 instead of showing the entire process flow.

3.1. Sacrificial release process

For nearly a decade from 1993 to 2003 we used process flows based on standard surface micromachining, particularly on sacrificial release. A variety of the sacrificial release processes have been published based on the same basic principle of forming a cavity underneath a thin plate by first depositing or growing a sacrificial layer on the carrier substrate and then selectively removing the sacrificial layer using an appropriate etchant, specifically chosen to etch the sacrificial layer material but not to etch the plate layer (Fig. 1.a) [Ergun05]. Different sacrificial layer, plate, and substrate material combinations have been used to fabricate CMUTs. An extended version of this process includes through-wafer via interconnections from the front side of the substrate to the backside. Deep reactive ion etching (DRIE) enables a dense array of high-aspect ratio vias in silicon that are filled with conductive material such as doped polysilicon to provide electrical connectivity from the front to the back of the substrate [Cheng02]. The major shortcoming of the sacrificial release process is the poor control over the uniformity, absolute thickness, and mechanical properties of deposited layers affecting important device parameters such as the gap height, the plate thickness, and the residual stress [Lin07].

3.2. Wafer bonding process

To improve on the process control and repeatability issues limiting the sacrificial release process and to reduce the process complexity, we developed a wafer bonding based process to fabricate CMUTs. A number of variations on the bonding process are listed below with continuing enhancement in performance.

3.2.1. Simple wafer bonding—This process begins with two wafers: a prime quality silicon wafer and a silicon-on-insulator (SOI) wafer. The cavity is defined on the prime wafer by selectively etching thermally grown oxide down to the substrate followed by a second thermal oxidation to grow the insulation layer. Following an RCA clean and surface activation, the SOI wafer and the prime wafer are brought together in vacuum. The wafers are then immediately annealed at high temperature (~1100°C) to form strong covalent bonds. The handle portion and the buried oxide layer of the SOI wafer are later removed, leaving a thin single crystal silicon plate suspended over the cavities. Finally electrical connections to the substrate are provided through openings in the oxide layer and individual elements are defined by etching isolation trenches in the silicon plate (Fig. 1.b) [Huang03]. To provide electrical connection to each element in a 2-D array from the backside of the substrate we also developed an interconnect technology compatible with the wafer bonding process. In this approach deep trenches etched in the silicon substrate define silicon pillars that serve as the individual interconnects to each element [Zhuang06]. The most important improvement enabled by wafer-bonding process is that the thickness, uniformity, and mechanical properties of the plate are well controlled thanks to the single crystal silicon device layer of the SOI wafer. This process also provides improved control over the gap height since it is mainly defined by thermal oxidation. However, the minimum gap height is limited by the thickness of the initial oxide layer. As a result, this structure is compromised

by reduced breakdown voltage and increased parasitic capacitance in the area between the cells of the CMUT. Another drawback in the described approach is related to the trench-isolated interconnect structure, which is prone to electrical short circuits due to possible contamination both on the front and backsides of the devices that might occur in subsequent packaging steps.

3.2.2. LOCOS process—An extended insulation layer structure in the post area would address the low breakdown voltage and high parasitic capacitance issues associated with the first-generation wafer-bonded CMUTs described in the previous subsection [Kupnik07]. We used the local oxidation of silicon (LOCOS), a widely used process step in standard IC processing, to form the extended post region (Fig. 1.c) [Park08]. This process also features an excellent gap height control achieved by patterning the silicon substrate inside the cavity via thermal oxidation, and then forming the oxide posts by a selective thermal oxidation step using the conventional LOCOS process. We demonstrated devices fabricated using this approach for chem/bio sensor applications [Lee10], but have not used this process for 2-D imaging arrays that would require a compatible through-wafer interconnect technology.

3.2.3. Thick-buried-oxide process—More recently we developed a structure and the associated process flow that confines and isolates the CMUT bottom electrode only to the region under the gap where the high electric field is desired [Kupnik10], so that the probability of dielectric breakdown and parasitic capacitance in the post region can be minimized. This structure also includes through-wafer via interconnects for accessing each element from the backside. The key component in this approach is an SOI wafer with a thick buried oxide layer. Vertical insulation trenches are used on the device layer of this SOI wafer to form completely insulated silicon bottom electrodes below the active plate region in each CMUT cell. The hot electrode is provided through an opening in the thick buried oxide layer filled by using doped polycrystalline silicon or any other electrically conductive material (Fig. 1.d). This arrangement provides each cell with its own individual connection to the hot electrode.

3.2.4. Piston-CMUT structure and process—We have developed other variations of the described basic device structures and process flows for various performance improvements. One such improvement is related to engineering the plate profile to approximate the membrane motion to an ideal piston-like motion. We have shown an improved transmit and receive performance, and wider fractional bandwidth using a plate structure with an added center mass compared to a classical CMUT structure with uniform membrane thickness (Fig. 1.e) [Huang09]. Such a structure can be implemented by forming the central mass by etching the device layer of an SOI layer or by plating metal on top of the plate structure. Another recent improved device structure we developed is based on a rigid plate connected to a substrate using relatively long and narrow posts, providing the spring constant for the movement of the plate (Fig. 1.f) [Nikoozadeh10A]. The resulting plate motion resembles that of an ideal piston. This structure not only improves the average displacement but also results in a significantly improved fill factor because the non-active plate anchor areas that is inevitable in a conventional CMUT structure is eliminated in this case. Both the added central mass and the compliant post approaches also separate the mass and spring components of the transducer and enable a more flexible design space.

4. Integration with electronic circuits

Close integration of ultrasonic transducer arrays and supporting integrated circuits is highly desired in many applications, especially for transducer arrays with small elements such as in 2-D arrays and arrays for use at the end of a catheter. In current conventional ultrasonic imaging systems, the array is located in a hand-held probe, which is connected to the main

processing unit via a cable bundle. Transmit pulsers and receive amplifiers are located in the main processing unit. Because of the small size and small capacitance of transducer elements in a 2-D array (piezoelectric or capacitive), the receiver electronics must be close to the transducer array, so that the additional capacitance introduced by the cable would not degrade the signal quality. Furthermore, multiplexing and beamforming circuitry can also be integrated with the array to minimize the number of active electronic channels and the number of physical connections between the probe and the backend system.

For integrating CMUT arrays with electronic circuits several methods developed for a variety of microelectro-mechanical systems (MEMS) applications have been adapted. These methods can be categorized in two main groups: monolithic and multi-chip (hybrid) approaches. Monolithic integration is realized by building CMUTs and electronics concurrently, or by building CMUTs on finished electronics wafers. For multichip (hybrid) integration, an integrated circuit die and a CMUT die can be directly bonded on top of each other or a flexible or rigid intermediate substrate may be used.

4.1. Monolithic integration

4.1.1. Co-processing—One method to monolithically integrate CMUTs and electronic circuits is to fabricate both components concurrently using a standard or minimally modified process. A BiCMOS process using 16 masks has been used with only minor modifications including an additional photolithography step and sacrificial layer etching to fabricate CMUTs side-by-side with electronic circuits on the same substrate [Eccardt97]. Although this method offers a cost-effective means of integration, it has two major limitations: 1) the transducer element area is shared by electronic circuits or interconnects. 2) The device dimensions in the vertical direction are limited by the film thicknesses available in the process used to make electronic circuits.

4.1.2. Post-processing by low-temperature surface micromachining—A second monolithic integration technique is to fabricate the electronic circuits first using a standard foundry process and then build CMUTs on top of finished electronics by further processing. This post-processing is kept minimal in a process called ‘CMUT-in-CMOS’ by augmenting a standard foundry process only with two blanket post-process steps for sacrificial etching and cavity sealing [Cheng09]. Although this process is fairly simple, it still suffers from the limitations on the device dimensions in the vertical direction because layers available in the standard foundry process are utilized as sacrificial layer. More complicated processing including surface passivation, planarization, opening of contacts to electronics, and further successive thin film deposition and etching steps is also demonstrated to define the CMUT plates with greater precision and control [Noble02, Daft04, Gurun08]. This approach has good area utilization and more control over device dimensions. However, processing techniques for making CMUTs are still limited, mainly due to temperature constraints set by the existing metal lines on the electronics.

4.1.3. Post-processing by low-temperature direct wafer bonding—We have recently demonstrated CMUTs fabricated by low temperature wafer bonding indicating that CMUTs can be directly built on a finished CMOS substrate by wafer bonding [Tsuji10]. This approach brings the advantages of the wafer bonding process such as control over the plate thickness, and process simplicity and provides a monolithic integration solution without going through the complexity of post-CMOS sacrificial release process explained in Section 4.1.2. In this low-temperature bonding process we used a thin titanium layer for electrical via-contact to CMOS substrate as well as an adhesion layer for wafer bonding. The gap height is set by the total thickness of the titanium adhesion layer and the passivation layer on the CMOS wafer.

4.2. Multichip integration

4.2.1. Chip-to-chip bonding—One can optimize fabrication processes for both CMUTs and frontend integrated circuits by making both components on separate substrates. In this case, CMUTs need through-wafer via interconnections from the front side of the substrate to the backside as explained in Section 3. CMUT arrays can then be bonded directly on electronics using well-established flip-chip bonding processes [Wygant08]. Direct bonding usually requires that the electronics die area to be greater than the CMUT die area, so that peripheral pads on the electronics die will be accessible to provide connections between the frontend circuits and the backend system.

4.2.2. Bonding on intermediate substrates—Using an intermediate substrate makes the size of the CMUT and electronics dice independent and could be desirable in the following cases: 1) In standard IC processing a reticle is stepped across a whole wafer to transfer the reticle image pattern to adjacent areas on the wafer. The reticle size limits the maximum size of a chip. Therefore, to implement very large CMUT arrays, electronics or both electronics and the CMUT array should be implemented by tiling several unit blocks. This approach also helps improve the overall yield one can achieve. A large array was recently demonstrated with several 16×16 2-D CMUT arrays flip-chip bonded on one side of a rigid interposer and several application specific integrated circuits (ASIC) bonded on the other side [Wodnicki09]. In a similar fashion we also demonstrated a rigid interposer with a single 32×32 2-D CMUT array on one side and four custom 16×16 ASICs on the other side (Fig. 2.a). In both demonstrations the interposer provides the electrical connections between the CMUT array and the electronics and also to the external backend system. 2) Using a flexible intermediate substrate the overall form factor of an integrated ultrasound probe can be minimized. We used this approach by folding an eight-legged flex circuit where each leg had a flip-chip bonded 8-channel frontend IC to address a 64-element CMUT ring array for forward-looking catheter-based intracardiac imaging (Fig. 2.b). Using this approach we were able to interface a CMUT array with 3-mm^2 silicon area with electronic circuits occupying a total area of 8-mm^2 silicon without increasing the final catheter size.

5. Imaging applications

Ultrasound is a non-ionizing radiation, and hence is well accepted for diagnostic use even in obstetrical applications. The image presentation is in real time, allowing the study of moving internal structures. Ultrasonic imaging equipment is cost-effective and portable. All these features have made ultrasound a widely used imaging modality in medicine. Ultrasound is particularly useful in imaging cardiac structures, the vascular system, the fetus and uterus, abdominal organs such as the liver, kidneys and gall bladder, and the eye. In this section, we present imaging results obtained using CMUT arrays in different shapes and forms to demonstrate the potential of CMUT technology for several diagnostic and therapy guiding applications.

5.1. Conventional 2-D cross-sectional imaging

Today, the most common form of ultrasonic transducers used for medical imaging is the 1-D array, which allows electronic focusing and steering of ultrasonic beams within an azimuthal plane resulting in 2-D cross-sectional images. We have built 1-D CMUT arrays of equivalent size, channel count, and operating frequency to state-of-the-art medical arrays employing piezoelectric transducers. Early versions of these arrays were fabricated using sacrificial release process and contained 128 individually addressable elements, each 6 mm high by 200 μm wide, with an element pitch of 250 μm. The experimental imaging results were in excellent agreement with the simulations, thus confirming the near ideal response of these transducer arrays [Oralkan02]. More recently, we have fabricated 128-element 1-D

arrays using the wafer bonding process. These arrays have a 300-μm-element pitch, are 3.3 mm long in the elevation direction and operate at a center frequency of 7.5 MHz with 100% fractional bandwidth (Fig. 3). 1-D CMUT arrays that we fabricated using the wafer-bonding technology were also used with commercial scanners to obtain clinical images [Mills03]. Compared to equivalent piezoelectric transducer arrays, CMUT arrays demonstrated an improved resolution and as a result better definition of fine structures in the carotid artery and the thyroid gland. More recently, Hitachi Corporation announced the first successful commercialization of a CMUT-based 1.5-D array for conventional 2-D cross-sectional imaging, manifesting the level of maturity CMUT technology has reached [Hitachi09].

5.2. 3-D Imaging using 2-D arrays

A 2-D transducer array allows electronic focusing and steering of ultrasonic beams both in azimuthal and elevational directions to enable real-time 3-D imaging. Progress in this field has been slow due to several challenges such as manufacturing large 2-D arrays with thousands of elements, providing front-end integrated circuits to preserve the signal integrity from very small transducer elements, dealing with a large number of electronic channels, and processing a large amount of data in real time. Recently, several major ultrasound system manufacturers have introduced 2-D array based 3-D imaging platforms to the market. These systems employ electronic multiplexing and beamforming circuitry next to the transducer array to reduce the number of active electronic channels [Savord03], so that standard backend systems with limited number of channels, i.e., 128-256 channels, can be used for image formation. The currently commercially available 2-D arrays consist of 2000-3000 elements fabricated from expensive materials such as single crystal piezoelectrics.

CMUT technology is especially promising for realization of large 2-D arrays that can be lithographically defined. As early as 1999, we demonstrated a 128×128-element 2-D array where each element was electrically accessible from the backside with a through-wafer via interconnects. Our first 3-D imaging results were obtained using a 8×16 element portion of this array flip-chip bonded to a fan-out die used along with the PC-based data acquisition system designed for 1-D CMUT arrays [Oralkan03]. Following this work, we developed a volumetric ultrasound imaging system based on a 16×16-element, 250-μm pitch 2-D CMUT array for 3-D endoscopic imaging. The array was flip-chip bonded to a custom IC that comprises the front-end electronics (Fig. 4.a). An output pressure of 330 kPa for a 25-V unipolar pulse and a minimum detectable pressure of 1 mPa/$\sqrt{\text{Hz}}$ were measured for the integrated prototype operating at a center frequency of 3 MHz. Using this system, we obtained volumetric images of a wire phantom (Fig. 4.b) and a vessel phantom. Although every element has its own dedicated pulser and amplifier, only a single element was selected at a time to simplify the initial implementation of this first-generation frontend IC, as discussed earlier. Thus, classic synthetic aperture image reconstruction was used [Wygant08]. We also demonstrated real-time images with a second-generation frontend IC we designed with transmit beamforming capability (Fig. 5.a) [Wygant09]. A nylon wire phantom (Fig. 5.b) and a left atrial model of the heart made of latex were imaged using the described 2-D CMUT array integrated with this second-generation IC. Currently, we are integrating four frontend ICs with a 32×32-element 2-D array using an interposer as explained in Section 4 to improve the image resolution.

5.3. Catheter-based imaging

Forward-viewing ultrasound volume images are desired for many intravascular and intracardiac applications such as guiding treatment of chronic total occlusion, helping stent deployment, and monitoring ablation procedures in the heart. An annular ring is the preferred geometry for transducer arrays because it can provide a 3-D volume image without

the complexity of a fully populated 2-D array. However, it is very challenging to implement this geometry in a very small scale (1-2 mm) using the existing piezoelectric transducer technology [Wang02]. On the other hand, CMUT arrays can be made in any arbitrary geometry with very small dimensions using photolithographic techniques and standard microfabrication processes. We have recently built a 12-F (4-mm diameter) intracardiac echo (ICE) catheter employing a 64-element CMUT ring array and eight 8-channel frontend ICs, all flip-chip bonded on a flex circuit placed at the tip of the catheter (Fig. 6.a). We used this catheter along with a programmable backend imaging system (Verasonics, Redmond, WA) to reconstruct real-time images of several imaging phantoms (Fig. 6.b) [Nikoozadeh10]. We have also built a 9-F (3-mm diameter) ICE catheter employing a 24-element, 65-μm pitch, 1-D microlinear array and a 24-channel frontend IC, flip-chip bonded on opposite sides of a flex circuit placed at the tip of a catheter (Fig. 7.a). In both types of catheters the electrical connectivity between the distal and proximal ends of the catheter were provided by a bundle of 48-AWG microcoaxial cables. We used this forward-looking microlinear catheter in-vivo to image a porcine heart model (Fig. 7.b) [Nikoozadeh10B]. These catheters demonstrate how miniature transducer arrays with integrated electronics are enabled by CMUT technology, especially critical for catheter-based imaging applications. The ring catheter is especially a powerful tool because of the volumetric imaging capability and the central lumen it provides to introduce other therapeutic tools during interventions.

5.4. Functional photoacoustic imaging

Photoacoustic imaging is a promising and emerging medical imaging modality providing functional information by combining the contrast information of optical imaging with the spatial resolution of acoustic imaging. In photoacoustic imaging, the target tissue is illuminated with short laser pulses that cause brief heating of absorbing structures such as blood vessels. The induced temperature increase generates acoustic pressure waves because of the thermoelastic effect. These pressure waves propagate to the surface of the tissue where they can be detected with ultrasound transducers. Photoacoustic imaging has typically relied on a single mechanically scanned focused piezoelectric transducer for detection of the laser-generated ultrasound. Using a 2-D CMUT array in place of a mechanically scanned element has a number of advantages. 3-D images can be acquired in one shot using large, two-dimensional arrays, which can be reliably fabricated using CMUT technology. To demonstrate the potential of CMUTs for photoacoustic imaging we performed a series of experiments [Vaithilingam09]. We used the 16×16-element 2-D CMUT array described in Section 5.2 to image indocyanine green (ICG) and blood filled polyethylene tubes embedded in chicken breast tissue [Fig. 8(a)]. We used double-sided laser illumination at a wavelength of 775 nm to gather the photoacoustic data since the peak ICG absorption is at this wavelength for the concentrations used. The 16×16 CMUT array and tank were mounted on a precision x-y translational stage to enable planar scanning and emulation of a 64 × 64 element CMUT array. An image reconstructed from this data is equivalent to that of an image reconstructed using a 64 × 64 element CMUT array. The pulse-echo and photoacoustic are shown in Fig. 8(b) and (c), respectively. The ability to obtain simultaneous pulse-echo and photoacoustic images enable to get both anatomical and functional images at once. Recently, we demonstrated the photoacoustic imaging depth could be extended up to 5 cm without exceeding the permitted laser exposure limit (20 mJ/cm^2 per pulse) mainly enabled by the superior noise performance of 2-D arrays with integrated frontend circuits [Ma10].

6. Therapeutic applications

Ultrasound is widely used as a diagnostic imaging modality in many clinical applications and has recently received increased attention and acceptance as a therapeutic tool. A significant advantage of using high intensity focused ultrasound (HIFU) over other

modalities, e.g. radio-frequency (RF) ablation, is the ability to generate a precise ablation pattern deep in tissue, with no effect on the surrounding structures. Today most HIFU systems in use employ spherical shell focused transducers operating in the range of 1 - 4 MHz and are based on piezoelectric materials such as PZT-8 and PZT-4 [Ebbini99]. More recently, phased array applicators were developed for HIFU. Phased arrays offer improved control features that are needed for precise lesion formation at a depth in the presence of tissue inhomogeneity and patient/applicator movement. Use of large arrays also enables the delivery of high acoustic power to the target area without generating high intensities on the surface of the transducer. As a result, the ultrasound energy passes harmlessly through overlying tissues en route to a tightly focused target area. HIFU applications can greatly benefit from the CMUT technology because of the ability to make large transducers arrays using basic microlithographic techniques. CMUTs also do not suffer from self-heating effects because they have much less internal loss compared to their piezoelectric counterparts and generated heat can be easily dissipated since they are fabricated from highly thermally conductive silicon. This makes CMUTs well suited for high power and continuous wave (CW) applications like HIFU. Our preliminary experimental results showed that CMUTs can be used in CW operation for extended periods of time, e.g., > 90 min, while producing acoustic pressures around 2 MPa peak-to-peak on the surface [Wong08, Wong10]. One of the most important design criteria for HIFU CMUTs is the current handling capability. Using thick doped silicon membranes and additional metal traces the Ohmic losses are minimized to avoid device failure by electromigration or self-heating. On the contrary to a common misconception plate fatigue is not a major failure mechanism in HIFU CMUTs. First, the deflection needed to obtain 1MPa at 10 MHz is only 10 nm. Second, even with other types of MEMS devices such as the digital micromirror devices with +/− 10 degree hinge movement, $>10^{12}$ cycles of operation have been demonstrated [Dougless98]. The reason for fatigue not being a major source of failure in small structures is that the accumulation of density of dislocations is not large enough to form fatigue related cracks. The macroscopic model for fatigue, which is based on dislocations piling up at the surface of a material and this way creating stress concentrations at sharp corners and scratches, does not hold for small structures.

We fabricated CMUT arrays specifically designed for HIFU applications using a high temperature direct fusion bonding process. Using one of the unfocused 2.5-MHz CMUT transducers with a size of 2.5 mm by 2.3 mm, we demonstrated heating in a gel phantom with unfocused ultrasound by 14-18°C over a 2.5-5 min time. The heating produced a ‘Cumulative Equivalent Minutes at 43°C (CEM43)’ of over 128 min in a sizeable volume. This is the threshold necrosis value for cardiac tissue. This experiment indeed shows that this device delivers output pressures needed for HIFU applications, and that it could potentially necrose a sizeable volume of cardiac tissue to a depth of approximately 1 cm. The acoustical to electrical efficiency of the CMUT used in this study was measured as 68% [Wong08].

7. Conclusion

The history of CMUTs is now approaching two decades. From being an interesting and efficient air transducer, now the CMUT is considered as a major platform technology to realize many medical diagnostic and therapeutic devices. In the last decade by concentrating on the close integration of CMUTs with supporting electronic circuits we demonstrated many miniature imaging devices and supporting systems for endoscopic and intracardiac imaging. Although the potential of CMUTs for diagnostic imaging is well understood, the potential for therapeutic applications in some measure is not fully explored. As a result one of the important future research directions in this field will be using CMUTs for integrated multimodal imaging and therapy. Another emerging application field that has not been

covered in this paper is sensing, in particular using CMUTs for medical sensor applications based on the principles of mass loading and acoustic wave propagation. In parallel with this expansion of the application field, there will be also many improvements on the device structures and fabrication processes to turn this exciting research field in to a complete commercial success. Some of the ongoing efforts in this direction include developing new device structures to achieve higher acoustic pressures in transmit using low to moderate level of electrical excitations, improving the electrical reliability, and increasing the level of integration with electronic circuits. However, as the recent introduction of CMUT-based imaging probes in to the market suggests, the complete commercial success of CMUT technology depends more on finding applications with high volume markets, rather than overcoming technological hurdles.

Acknowledgments

This work was supported by the National Institutes of Health under grants CA99059, CA134720, and HL67647.

References

[Haller94]. Haller, MI.; Khuri-Yakub, BT. A surface micromachined electrostatic ultrasonic air transducer. Proc. IEEE Ultrason. Symp.; 1994. p. 1241-1244.

[Hitachi09]. www.hitachi-medical.co.jp/medix/pdf/vol51/P31-34.pdf

[Jin98]. Jin X, Ladabaum I, Khuri-Yakub BT. The microfabrication of capacitive ultrasonic transducers. IEEE/ASME J. Microelectromech. Syst. Sep..1998 vol. 7:295–302.

[Jin99]. Jin X, Ladabaum I, Degertekin FL, Calmes S, Khuri-Yakub BT. Fabrication and characterization of surface micromachined capacitive ultrasonic immersion transducers. IEEE/ASME J. Microelectromech. Syst. Mar..1999 vol. 8:100–114.

[Schindel95]. Schindel DW, Hutchins DA. The design and characterization of micromachined air-coupled capacitance transducers. IEEE Trans. Ultrason., Ferroelect., Freq. Contr. Jan..1995 vol. UFFC-42:42–50.

[Haller96]. Haller MI, Khuri-Yakub BT. A surface micromachined electrostatic ultrasonic air transducer. IEEE Trans. Ultrason., Ferroelect., Freq. Contr. Jan..1996 vol. UFFC-43:1–6.

[Eccardt96]. Eccardt, PC.; Niederer, K.; Scheiter, T.; Hierhold, C. Surface micromachined ultrasound transducers in CMOS technology. Proc. IEEE Ultrason. Symp.; 1996. p. 959-962.

[Eccardt97]. Eccardt, PC.; Niederer, K.; Fischer, B. Micromachined transducers for ultrasound applications. Proc. IEEE Ultrason. Symp.; 1997. p. 1609-1618.

[Cianci02]. Cianci E, Foglietti V, Caliano G, Pappalardo M. Micromachined capacitive ultrasonic transducers fabricated using silicon on insulator wafers. Microelectronic Engineering. Jul..2002 vol. 61-62:1025–1029.

[Huang03]. Huang Y, Ergun AS, Haeggström E, Badi MH, Khuri-Yakub BT. Fabricating capacitive micromachined ultrasonic transducers with wafer-bonding. IEEE/ASME J. Microelectromech. Syst. Apr.; 2003 vol. 12(no.2):128–137.

[Ladabaum98]. Ladabaum I, Jin X, Soh HT, Atalar A, Khuri-Yakub BT. Surface micromachined capacitive ultrasonic transducers. IEEE Trans. Ultrason., Ferroelect., Freq. Contr. May.1998 vol. 45:678–690.

[Caronti02]. Caronti A, Caliano G, Iula A, Pappalardo M. An accurate model for capacitive micromachined ultrasonic transducers. IEEE Trans. Ultrason., Ferroelect., Freq. Contr. Aug.. 2002 vol. 49:159–168.

[Lohfink05]. Lohfink A, Eccardt P-C. Linear and nonlinear equivalent circuit modeling of CMUTs. IEEE Trans. Ultrason., Ferroelect., Freq. Contr. Dec..2005 vol. 52:2163–2172.

[Bozkurt99]. Bozkurt A, Ladabaum I, Atalar A, Khuri-Yakub BT. Theory and analysis of electrode size optimization for capacitive microfabricated ultrasonic transducers. IEEE Trans. Ultrason., Ferroelect., Freq. Contr. Nov..1999 vol. 46:1364–1374.

[Wojcik00]. Wojcik, G.; Mould, J.; Reynolds, P.; Fitzgerald, A.; Wagner, P.; Ladabaum, I. Time-domain models of MUT array cross-talk in silicon substrates. Proc. IEEE Ultrason. Symp.; 2000. p. 909-914.

[Roh02]. Roh Y, Khuri-Yakub BT. Finite element analysis of underwater micromachined ultrasonic transducers. IEEE Trans. Ultrason., Ferroelect., Freq. Contr. Mar..2002 vol. 49:293–298.

[Yaralioglu05]. Yaralioglu GG, Ergun AS, Khuri-Yakub BT. Finite-element analysis of capacitive micromachined ultrasonic transducers. IEEE Trans. Ultrason., Ferroelect., Freq. Contr. Dec.; 2005 vol. 52(no. 12):2185–2198.

[Bayram07]. Bayram B, Kupnik M, Yaralioglu GG, Oralkan Ö, Ergun AS, Lin D, Wong SH, Khuri-Yakub BT. Finite element modeling and experimental characterization of crosstalk in 1-D CMUT arrays. IEEE Trans. Ultrason., Ferroelect., Freq. Contr. Feb.; 2007 vol. 54(no. 2):418–430.

[Oralkan99]. Oralkan Ö, Jin X, Degertekin FL, Khuri-Yakub BT. Simulation and experimental characterization of a 2-D capacitive micromachined ultrasonic transducer array element. IEEE Trans. Ultrason., Ferroelect., Freq. Contr. Nov..1999 vol. 46:1337–1340.

[Jin01]. Jin X, Oralkan Ö, Degertekin FL, Khuri-Yakub BT. Characterization of one-dimensional capacitive micromachined ultrasonic immersion transducer arrays. IEEE Trans. Ultrason., Ferroelect., Freq. Contr. May.2001 vol. 48:750–760.

[Oralkan02]. Oralkan Ö, Ergun S, Johnson JA, Karaman M, Demirci U, Kaviani K, Lee TH, Khuri-Yakub BT. Capacitive micromachined ultrasonic transducers: Next-generation arrays for acoustic imaging? IEEE Trans. Ultrason., Ferroelect., Freq. Contr. Nov..2002 vol. 49:1596–1610.

[Oralkan03]. Oralkan Ö, Ergun AS, Cheng CH, Johnson JA, Karaman M, Lee TH, Khuri-Yakub BT. Volumetric ultrasound imaging using 2-D CMUT arrays. IEEE Trans. Ultrason., Ferroelect., Freq. Contr. Sep.; 2003 vol. 50(no. 11):1581–1594.

[Lin10]. Lin D-S, Zhuang X, Wong SH, Kupnik M, Khuri-Yakub BT. Encapsulation of capacitive micromachined ultrasonic transducers using viscoelastic polymer. IEEE/ASME J. Microelectromech. Syst. Dec.; 2010 vol. 19(no. 6):1341–1351.

[Ergun05]. Ergun AS, Huang Y, Zhuang X, Oralkan Ö, Yaralioglu GG, Khuri-Yakub BT. Capacitive micromachined ultrasonic transducers: fabrication technology. IEEE Trans. Ultrason., Ferroelect., Freq. Contr. Dec.; 2005 vol. 52(no.12):2270–2275.

[Cheng02]. Cheng, CH.; Ergun, AS.; Khuri-Yakub, BT. Electrical through wafer interconnects with 0.05 pico farads parasitic capacitance on 400 μm thick silicon substrate. Proc. North Amer. Solid-State Sensor, Actuator, and Microsystems Workshop; 2002. p. 157-160.

[Lin07]. Lin, DS.; Zhuang, X.; Wong, SH.; Ergun, AS.; Kupnik, M.; Khuri-Yakub, BT. Characterization of fabrication related gap-height variations in capacitive micromachined ultrasonic transducers. Proc. IEEE Ultrason. Symp.; 2007. p. 523-526.

[Zhuang06]. Zhuang, X.; Ergun, AS.; Oralkan, Ö.; Wygant, IO.; Khuri-Yakub, BT. Interconnection and Packaging for 2D Capacitive Micromachined Ultrasonic Transducer Arrays Based on Through-Wafer Trench Isolation. Proc. IEEE MEMS Conf.; 2006. p. 270-273.

[Kupnik07]. Kupnik, M.; Ergun, AS.; Huang, Y.; Khuri-Yakub, BT. Extended insulation layer structure for CMUTs. Proc. IEEE Ultrason. Symp.; 2007. p. 511-514.

[Park08]. Park, KK.; Lee, HJ.; Kupnik, M.; Oralkan, Ö.; Khuri-Yakub, BT. Fabricating capacitive micromachined ultrasonic transducers with direct wafer-bonding and LOCOS technology. Proc. IEEE MEMS Conf.; 2008. p. 339-342.

[Lee10]. Lee, H.; Park, KK.; Kupnik, M.; Oralkan, Ö.; Khuri-Yakub, BT. Highly sensitive detection of DMMP using a CMUT-based chemical sensor. Proc. IEEE Sensors Conf.; 2010. p. 2122-2126.

[Kupnik10]. Kupnik, M.; Vaithilingam, S.; Torashima, K.; Wygant, IO.; Khuri-Yakub, BT. CMUT fabrication based on a thick buried oxide layer. Proc. IEEE Ultrason. Symp.; 2010.

[Nikoozadeh10A]. Nikoozadeh, A.; Khuri-Yakub, PT. CMUT with substrate-embedded springs for non-flexural plate movement. Proc. IEEE Ultrason. Symp.; 2010.

[Huang09]. Huang Y, Zhuang X, Hæggstrom EO, Ergun AS, Cheng C-H, Khuri-Yakub BT. Capacitive micromachined ultrasonic transducers with piston-shaped membranes: Fabrication and experimental characterization. IEEE Trans. Ultrason., Ferroelect., Freq. Contr. Jan.; 2009 vol. 56(no. 1):136–145.

[Nikoozadeh10B]. Nikoozadeh, A.; Oralkan, Ö.; Gencel, M.; Choe, JW.; Stephens, DN.; de la Rama, A.; Chen, P.; Lin, F.; Dentinger, A.; Wildes, D.; Thomenius, K.; Shivkumar, K.; Mahajan, A.; Seo, CH.; O'Donnell, M.; Truong, U.; Sahn, DJ.; Khuri-Yakub, PT. Forward-looking intracardiac imaging catheters using fully integrated CMUT arrays. Proc. IEEE Ultrason. Symp.; 2010.

[Vaithilingam09]. Vaithilingam S, Ma T-J, Furukawa Y, Wygant IO, Zhuang X, de la Zerda A, Oralkan Ö, Kamaya A, Gambhir SS, Jeffrey RB Jr. Khuri-Yakub BT. Three-dimensional photoacoustic imaging using a two-dimensional CMUT array. IEEE Trans. Ultrason., Ferroelect., Freq. Contr. Nov.; 2009 vol. 56(no. 11):2411–19.

[Ma10]. Ma, T-J.; Kothapalli, SR.; Vaithilingam, S.; Oralkan, Ö.; Kamaya, A.; Wygant, IO.; Zhuang, X.; Gambhir, SS.; Jeffrey, RB., Jr.; Khuri-Yakub, BT. 3-D deep penetration photoacoustic imaging with a 2-D CMUT array. Proc. IEEE Ultrason. Symp.; 2010.

[Cheng09]. Cheng, X.; Lemmerhirt, DF.; Kripfgans, OD.; Zhang, M.; Yang, C.; Rich, CA.; Fowlkes, JB. CMUT-IN-CMOS ultrasonic transducer arrays with on-chip electronics. Proc. Int. Conf. Solid-State Sensors and Actuators; 2009. p. 1222-1225.

[Noble02]. Noble, RA.; Davies, RR.; King, DO.; Day, MM.; Jones, ARD.; McIntosh, JS.; Hutchins, DA.; Saul, P. Low temperature micromachined cMUTs with fully-integrated analogue front-end electronics. Proc. IEEE Ultrason. Symp.; 2002. p. 1045-1050.

[Daft04]. Daft, C.; Calmes, S.; da Graca, D.; Patel, K.; Wagner, P.; Ladabaum, I. Microfabricated ultrasonic transducers monolithically integrated with high voltage electronics. Proc. IEEE Ultrason. Symp.; 2004. p. 493-496.

[Gurun08]. Gurun, G.; Qureshi, MS.; Balantekin, M.; Guldiken, R.; Zahorian, J.; Sheng-Yu, P.; Basu, A.; Karaman, M.; Hasler, P.; Degertekin, L. Front-end CMOS electronics for monolithic integration with CMUT arrays: circuit design and initial experimental results. Proc. IEEE Ultrason. Symp.; 2008. p. 390-393.

[Tsuji10]. Tsuji, Y.; Kupnik, M.; Khuri-Yakub, BT. Low temperature process for CMUT fabrication with wafer bonding technique. Proc. IEEE Ultrason. Symp.; 2010.

[Iyer02]. Iyer, SS.; Herv'e, A. J. Auberton, editors. Silicon Wafer Bonding Technology for VLSI and MEMS Applications. INSPEC, The Institution of Electrical Engineers; London: 2002.

[Wygant08]. Wygant I, Zhuang X, Yeh D, Oralkan O, Ergun AS, Karaman M, Khuri-Yakub BT. Integration of 2D CMUT arrays with front-end electronics for volumetric ultrasound imaging. IEEE Trans. Ultrason., Ferroelect., Freq. Contr. Feb.; 2008 vol. 55(no. 2):327–342.

[Wodnicki09]. Wodnicki, R.; Woychik, CG.; Byun, AT.; Fisher, R.; Thomenius, K.; Lin, D-S.; Zhuang, X.; Oralkan, O.; Vaithilingam, S.; Khuri-Yakub, BT. Multi-row linear cMUT array using cMUTs and multiplexing electronics. Proc. IEEE Ultrason. Symp.; 2009. p. 2699-2699.

[Mills03]. Mills, DM.; Smith, LS. Real-time in vivo imaging with capacitive micromachined ultrasound transducer (CMUT) linear arrays. Proc. IEEE Ultrason. Symp.; 2003. p. 568-571.

[Wygant09]. Wygant, IO.; Jamal, NS.; Lee, HJ.; Nikoozadeh, A.; Oralkan, O.; Karaman, M.; Khuri-Yakub, BT. An integrated circuit with transmit beamforming flip-chip bonded to a 2-D CMUT array for 3-D ultrasound imaging; IEEE Trans. Ultrason., Ferroelect., Freq. Contr; Oct.. 2009 p. 2145-56.

[Wang02]. Wang Y, Stephens DN, O'Donnell M. Optimizing the beam pattern of a forward-viewing ring-annular ultrasound array for intravascular imaging. IEEE Trans. Ultrason., Ferroelect., Freq. Contr. 2002; vol. 49:1652–1664.

[Ebbini99]. Ebbini, ES.; Seip, R.; Vanbaren, P.; Haddadin, O.; Simon, C.; Botros, YY. Therapeutic Ultrasound. In: Webster, J., editor. Wiley Encyclopedia of Electrical and Electronics Engineering. John Wiley & Sons, Inc.; 1999.

[Wong08]. Wong SH, Watkins RD, Kupnik M, Butts-Pauly K, Khuri-Yakub BT. Feasibility of MR-Temperature Mapping of Ultrasonic Heating from a CMUT. IEEE Trans. Ultrason., Ferroelect., Freq. Contr. Apr.; 2008 vol. 55(no. 4):811–818.

[Wong10]. Wong SH, Kupnik M, Watkins RD, Butts-Pauly KB, Khuri-Yakub BT. Capacitive micromachined ultrasonic transducers for therapeutic ultrasound applications. IEEE Trans. Biomed. Eng. Jan.; 2010 vol. 57(no. 1):114–123. [PubMed: 19628448]

[Douglass98]. Douglass, MR. Lifetime Estimates and Unique Failure Mechanisms of the Digital Micromirror Device (DMD). Proc. IRPS; 1998. p. 9-16.

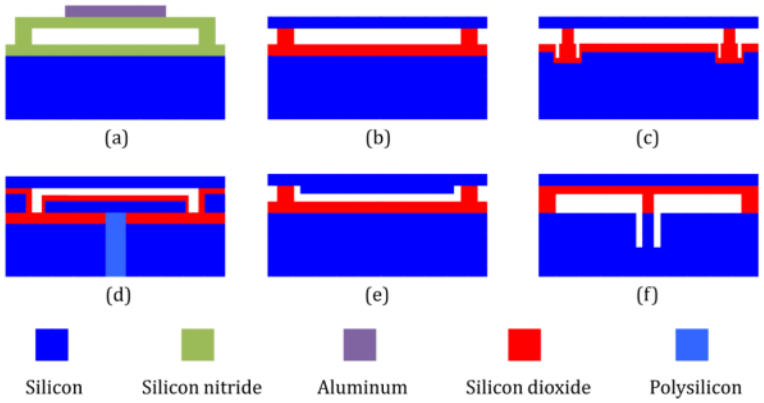

Fig. 1.

Schematic cross-sections for different CMUT structures. (a) CMUT fabricated using sacrificial release process. (b) CMUT fabricated using simple wafer bonding process. (c) CMUT fabricated using LOCOS process. (d) CMUT fabricated using the thick-buried-oxide process. (e) CMUT with added mass on its plate. (f) CMUT with the compliant post structure.

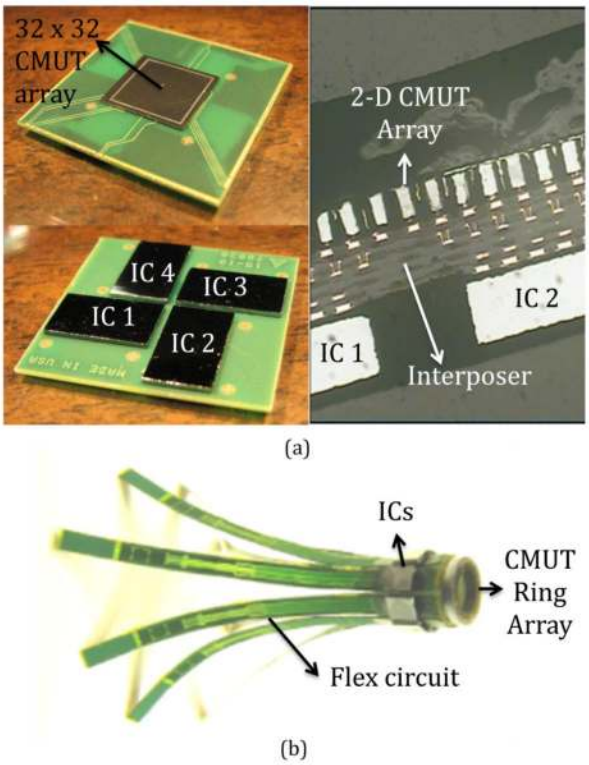

Fig. 2.

Multichip hybrid integration. (a) left panel top: A 32×32 2-D CMUT array flip-chip bonded on the top side of a rigid interposer. Left panel bottom: Four ICs flip-chip bonded on the bottom side of the interposer. Right panel: The cross-sectional view of the multichip assembly. (b) Eight ICs and a 64-element CMUT ring array flip-chip bonded on flexible printed circuit board. Each leg of the flexible PCB is folded for placement in the catheter tip.

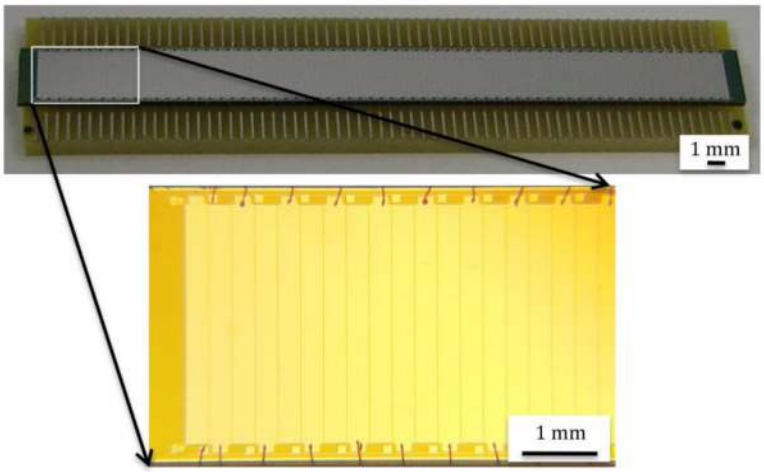

Fig. 3.
A 132-element 1-D CMUT array fabricated using the simple wafer bonding process.

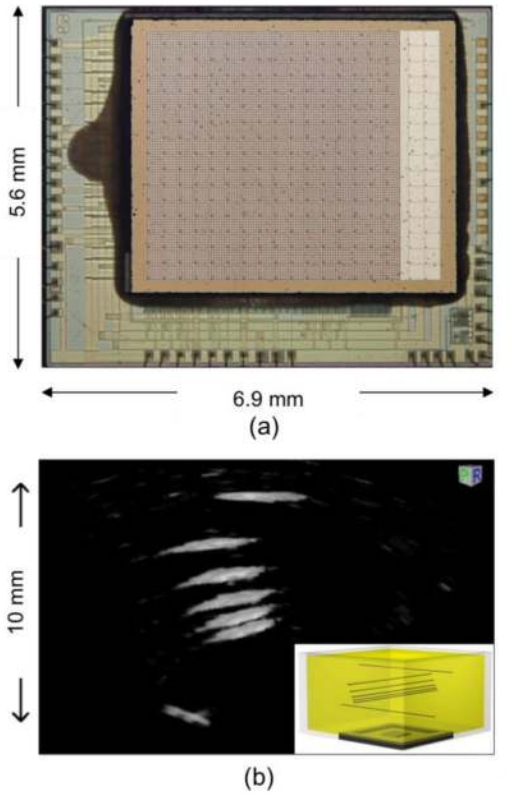

Fig. 4.
(a) A 16×16 2-D CMUT array flip-chip bonded on the first-generation custom frontend IC. (b) 3-D rendered image of a wire phantom obtained in synthetic aperture mode with a 5-MHz array (The phantom is schematically shown in the inset).

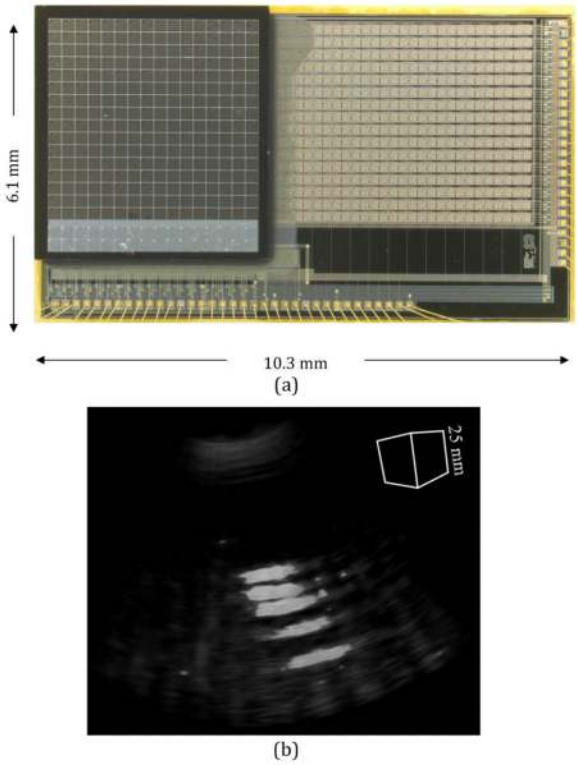

Fig. 5.
(a) A 16×16 2-D CMUT array flip-chip bonded on the second-generation custom frontend IC with transmit beamforming capability. (b) 3-D rendered image of a wire phantom with a 2.5-MHz array.

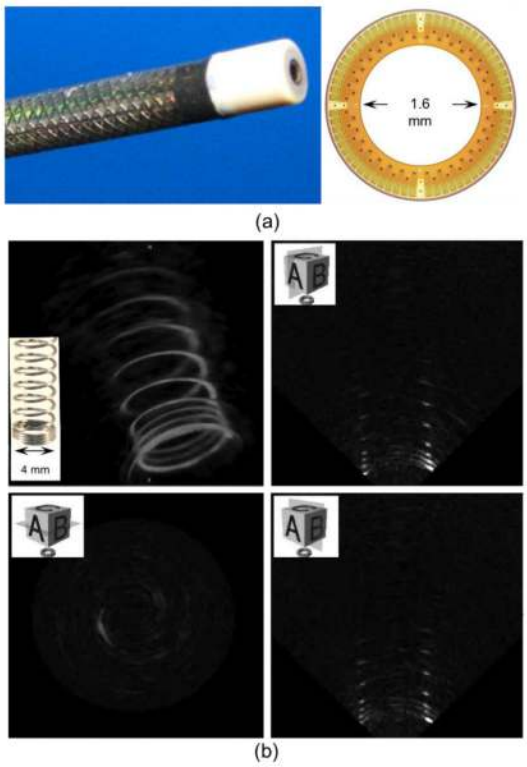

Fig. 6.
(a) Left panel: A 12-F forward-looking ring catheter. Right panel: A 64-element CMUT ring array. (b) The 3-D rendered image of a metal spring and three different cross-sectional images captured in real time.

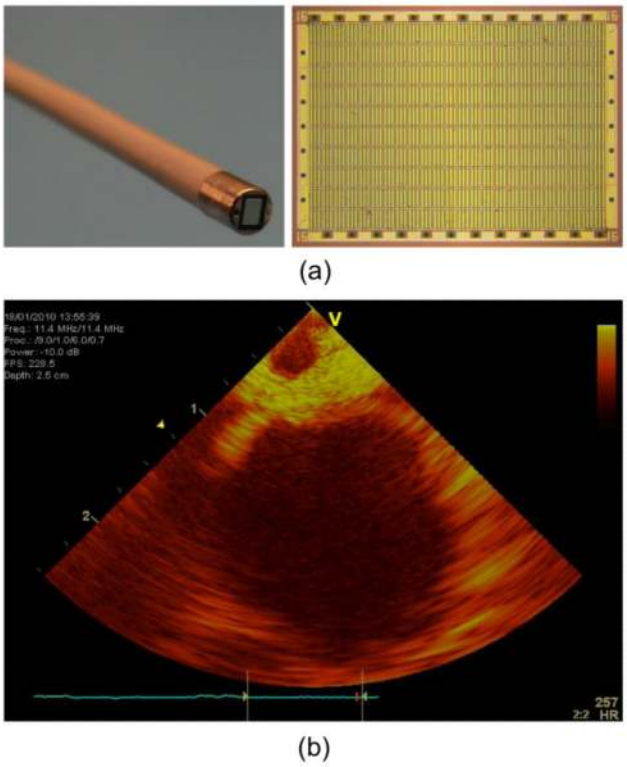

Fig. 7.
(a) Left panel: The 9-F forward-looking microlinear catheter. Right panel: A 24-element CMUT microlinear array. (b) A 2D image obtained with the CMUT microlinear array in-vivo in a pig heart.

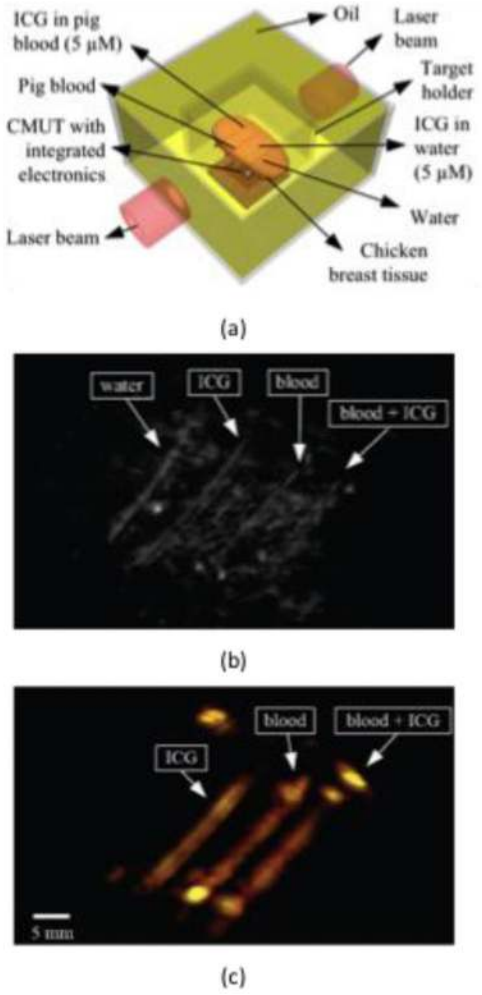

Fig. 8.

Photoacoustic images of the chicken breast phantom, reconstructed using the data from a 64 × 64 aperture. (a) Schematic of tubes embedded in chicken breast phantom. (b) 3-D rendered pulse-echo image (grayscale). (c) 3-D rendered photoacoustic image (red).